Original Article

Network pharmacology-guided investigation of Fuzheng Yanggan Huaxian decoction in a CCL₄-induced hepatic fibrosis mouse model: involvement of the TLR4-MAPK/NF-κB signaling axis and intestinal barrier

Jianguo Ma^{1*}, Xue Zang^{1*}, Xiang Li^{2,3*}, Min Xu⁴, Shenghua Zhang⁵, Xin Chen², Ting Zhu², Yunpeng Luan¹, Xia Chen¹, Yong Qiu²

¹The First Affiliated Hospital of Yunnan University of Chinese Medicine, Kunming 650021, Yunnan, China; ²Yunnan University of Chinese Medicine, Kunming 650500, Yunnan, China; ³Yunnan Provincial Clinical Medical Center for Chinese Medicine (Spleen and Stomach Diseases), Kunming 650021, Yunnan, China; ⁴Department of Spleen and Stomach Diseases, Yixing Hospital of Traditional Chinese Medicine, Yixing 214200, Jiangsu, China; ⁵Department of Spleen and Stomach Diseases, Affiliated Hospital of Traditional Chinese Medicine, Chongqing Three Gorges Medical College, Chongqing 404000, China. *Equal contributors and co-first authors.

Received May 17, 2025; Accepted July 22, 2025; Epub September 15, 2025; Published September 30, 2025

Abstract: Objective: This study employed a carbon tetrachloride (CCl₄)-induced hepatic fibrosis mouse model to investigate the therapeutic effects and mechanisms of Fuzheng Yanggan Huaxian Decoction (FZYGHX). Methods: Network pharmacology analysis was conducted to identify the Toll-like receptor 4 (TLR4)-mitogen-activated protein kinase (MAPK)/nuclear factor-kappa B (NF-κB) signaling pathway as a key regulatory axis, which was subsequently validated through in vivo experiments. Results: FZYGHX treatment preserved liver morphology, reduced serum aspartate aminotransferase and alanine aminotransferase levels, and mitigated histopathological damage. Histological assessments demonstrated improved liver architecture, reduced fibrosis, and suppressed collagen deposition. Mechanistically, FZYGHX attenuated hepatic inflammation by downregulating macrophage marker F4/80 and proinflammatory cytokines interleukin-6 and tumor necrosis factor-alpha. Furthermore, FZYGHX reinforced intestinal barrier function by upregulating tight junction (TJ) proteins (zonula occludens-1 (ZO-1), claudin-1, and occludin), while decreasing serum lipopolysaccharide (LPS) and hepatic LPS-binding protein (LBP) levels. The FITC-dextran assay confirmed restoration of mucosal barrier integrity. Conclusion: These findings suggest that the anti-fibrotic effects of FZYGHX are mediated, at least in part, by inhibition of the TLR4-MAPK/NF-κB pathway and enhancement of intestinal barrier function.

Keywords: Fuzheng Yanggan Huaxian decoction, hepatic fibrosis, TLR4-MAPK/NF-κB signaling pathway, network pharmacology

Introduction

Hepatic fibrosis arises from various etiologies, including viral hepatitis, autoimmune diseases, genetic and metabolic disorders, and exposure to chemical or toxic agents. These factors induce hepatocellular injury, triggering persistent inflammation and progressive fibrotic changes within the liver [1]. Key cytokines involved in liver fibrogenesis, such as tumor necrosis factor- α (TNF- α), interleukin-6 (IL-6), and interleukin-10 (IL-10), promote the activation of hepatic stellate cells (HSCs) into myofi-

broblasts, which subsequently overproduce extracellular matrix (ECM) components [2].

The liver receives dual blood supply, with approximately two-thirds of its afferent flow derived from the portal vein, which transports nutrient-rich blood from the intestines. This unique vascular anatomy renders the liver particularly susceptible to antigenic exposure from the gut. The integrity of the intestinal mucosal barrier depends largely on its mechanical structure, primarily composed of intestinal epithelial cells joined by TJs [3]. Disruption of TJs compro-

mises the barrier, resulting in widened intercellular spaces, increased paracellular permeability, and enhanced translocation of bacteria and endotoxins into the portal circulation [4].

Among these endotoxins, LPS is a key ligand that activates Toll-like receptor 4 (TLR4), expressed on the surface of HSCs. Upon entering the liver, LPS binds to TLR4 and initiates downstream signaling cascades, including the nuclear factor-kappa B (NF-kB) and mitogenactivated protein kinase (MAPK) pathways. These pathways play central roles in modulating inflammation, hepatocyte survival, Kupffer cell activation, and HSC transdifferentiation. The TLR4-MAPK/NF-kB axis thus serves as a crucial mechanistic bridge linking intestinal barrier dysfunction with hepatic inflammation, underscoring the therapeutic potential of guttargeted interventions in liver fibrosis [5].

Current pharmacological treatments for hepatic fibrosis are limited by adverse effects and inconsistent efficacy. Therefore, the development of effective and well-tolerated therapies to prevent progression to cirrhosis or hepatocellular carcinoma (HCC) remains an urgent clinical need. Traditional Chinese medicine (TCM), with a long history of empirical use, offers promising strategies for preventing and treating hepatic fibrosis. Fuzheng Yanggan Huaxian Decoction (FZYGHX), formulated by the renowned TCM practitioner Professor Long Zuhong based on the principle of "Therapeutic emphasis on spleen regulation is pivotal in managing liver disorders", has shown clinical efficacy in ameliorating hepatic fibrosis. However, its mechanisms of action require further clarification.

With the rapid advancement of bioinformatics and systems biology, network pharmacology has emerged as a powerful tool for elucidating the multicomponent and multitarget mechanisms of Chinese herbal medicines. Integrating these approaches into TCM research enables a shift from single-target analysis toward comprehensive mapping of compound-target networks, offering deeper mechanistic insights.

Building on this rationale, the present study investigated the anti-fibrotic effects of FZYGHX in a carbon tetrachloride (CCl₄)-induced hepatic fibrosis mouse model. Based on network pharmacology predictions, the study hypothe-

sized that FZYGHX modulates the TLR4-MAPK/NF-κB signaling pathway and protects intestinal barrier integrity. These mechanisms were subsequently validated through in vivo pharmacological experiments.

Materials and methods

Animals and experimental design

Adult male C57BL/6J mice (19-21 g) were obtained from Beijing HFK Bioscience Co., Ltd. [SCXK (Jing) 2019-0008] and housed under standard conditions (20-23°C, 40-60% humidity, 12-h light/dark cycle). All animal procedures adhered to national laboratory animal welfare guidelines and were approved by the Institutional Animal Care and Use Committee of Yunnan University of Traditional Chinese Medicine (Approval No. R-062022S051).

A total of 40 mice were randomly assigned to four groups (n=10 per group): control group, CCl₄ model group, low-dose FZYGHX group (FZYGHX-L group, 0.45 g/kg), and high-dose FZYGHX group (FZYGHX-H group, 1.8 g/kg). Gavage doses were calculated based on body surface area (BSA) scaling. The clinical dose of FZYGHX for a 60 kg adult is 132 g/day of crude herbs, equivalent to 2.2 g/kg. According to Food and Drug Administration guidelines [6], the mouse equivalent dose was calculated as:

Mouse dose (g/kg) = Human dose (g/kg) × (Mouse BSA coefficient/Human BSA coefficient).

Using BSA coefficients of 0.0071 (mouse) and 0.0173 (human), the equivalent dose in mice was approximately 0.9 g/kg. For a 20 g mouse, this corresponded to 18 mg/day of crude herb. Assuming a single gavage volume of 0.2 mL/mouse, the middle-dose concentration was 90 mg/mL. Low- and high-dose groups received 50% and 200% of this dose, respectively (0.45 g/kg and 1.8 g/kg). Dose safety was confirmed through preliminary toxicity tests, with no observed adverse effects.

After 7 days of acclimatization, the control group received intraperitoneal injections of olive oil (5 mL/kg, 3 times/week for 8 weeks). The other groups received 20% CCl₄ in olive oil (1:4 ratio, 5 mL/kg i.p., 3 times/week) for 8 weeks. Simultaneously, FZYGHX-L and FZY-GHX-H groups received daily oral gavage of

FZYGHX decoction (0.45 or 1.8 g/kg), while the control and model groups were given an equivalent volume of distilled water (10 mL/kg/day).

After 8 weeks, mice were anesthetized with pentobarbital (100 mg/kg i.p.), and serum samples were collected and stored at -80°C for biochemical analyses. Liver and colon tissues were excised for gross evaluation; portions were fixed in 10% formalin for histology or snap-frozen for molecular analyses. The hepatosomatic index was calculated as: liver weight/body weight × 100% (Figure 1A).

All surgical procedures were conducted under aseptic conditions. Analgesia was provided 30 minutes before surgery via intraperitoneal injection of buprenorphine (0.05 mg/kg). During partial hepatectomy, anesthesia was maintained using 2.5% isoflurane in oxygen via a nose cone, with respiratory rate and pedal reflexes monitored every 10 minutes. Postoperative analgesia (buprenorphine, 0.05 mg/ kg, every 12 h) was continued for 48 hours, along with subcutaneous saline (2 mL) to prevent dehydration. At study termination, euthanasia was performed using gradual CO2 inhalation (30% chamber volume displacement per minute), followed by cervical dislocation, in accordance with American Veterinary Medical Association guidelines. Environmental enrichment (e.g., nesting materials, social housing) and twice-daily health monitoring were implemented to minimize animal distress.

Preparation of FZYGHX decoction

The FZYGHX decoction consisted of 10 traditional Chinese medicinal herbs: Astragali Radix (20 g, YP20231101), Atractylodis Macrocephalae Rhizoma (15 g, 20230302), Artemisiae Scopariae Herba (10 g, 2312040), Coicis Semen (12 g, 20231101), Curcyrrhizae Rhizoma (10 g, C231208006), Salviae Miltiorrhizae Radix et Rhizoma (15 g, 231001), Raphani Semen (10 g, 24091211), Ostreae Concha (15 g, Y230501), Aurantii Fructus (10 g, YP20230101), and Glycyrrhiza uralensis Fisch (5 g, 230806). Details are summarized in Table 1.

The decoction was prepared using isodose granules produced by Tianjiang Pharmaceutical Co., which met quality control standards. The granules were reconstituted with distilled water

to yield different concentrations and stored at 4°C for oral administration.

Serum aminotransferases and hepatic hydroxyproline

Serum levels of alanine aminotransferase (ALT; Cat# C009-2-1) and aspartate aminotransferase (AST; Cat# C009-2-1) were measured using commercial kits from Nanjing Jiancheng Bioengineering Research Institute (Nanjing, China). Hepatic hydroxyproline (Hyp; Cat# A030-2-1), a marker of collagen deposition, was quantified in liver hydrolysates using a kit from the same supplier, following the manufacturer's instructions.

Inflammatory cytokine quantification

Liver tissues were homogenized (10% w/v) in ice-cold PBS (pH 7.4) and centrifuged at 3,000 rpm for 20 minutes at 4°C. Supernatants and serum samples were analyzed for TNF- α (Abbkine, KTE7015), IL-6 (Abbkine, KTE6017), and IL-10 (Abbkine, KTE7010) using enzyme-linked immunosorbent assay (ELISA) kits (Abbkine Scientific Co., Ltd., Wuhan, China), following the manufacturer's protocols. Cytokine concentrations in cell culture supernatants were assessed similarly.

Histology and immunohistochemistry

Liver and intestinal tissues were fixed in 10% neutral buffered formalin, embedded in paraffin, and sectioned at 4-5 µm. Hematoxylin and eosin (H&E) staining was performed for general histopathological evaluation, while Sirius red staining was used to assess collagen deposition [7]. Nuclei were counterstained with hematoxylin. Fibrosis severity was semiquantitatively graded using the METAVIR scoring system [8], with evaluation performed by two blinded pathologists under a Nikon Eclipse E200 light microscope.

Network pharmacology analysis

Active compounds in FZYGHX and their targets were identified using the Traditional Chinese Medicine Systems Pharmacology Database (TCMSP). Disease-related targets for hepatic fibrosis were retrieved from the OMIM, TTD, GeneCards, and DisGeNET databases. Overlapping targets between the compound and

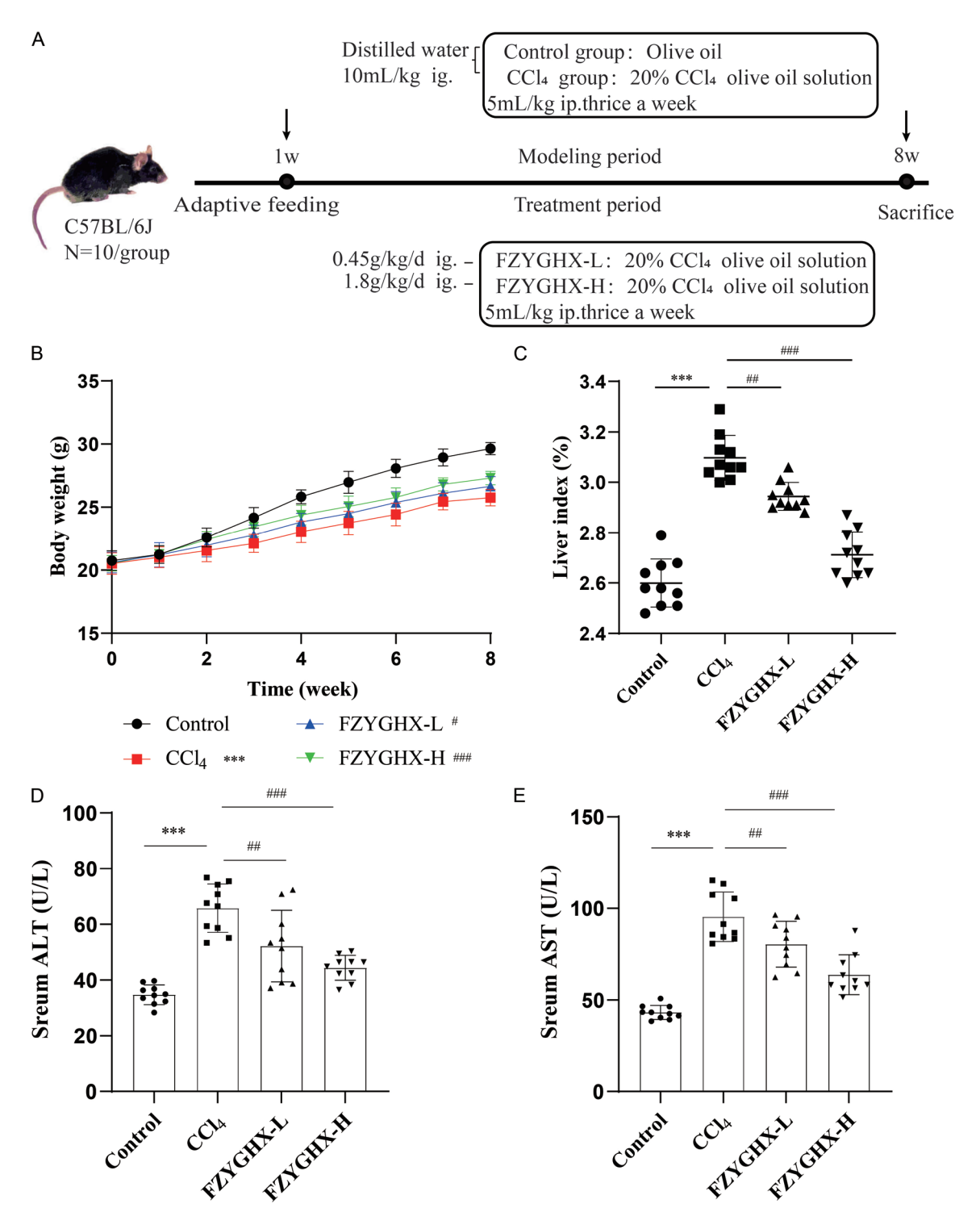


Figure 1. Fuzheng Yanggan Huaxian Decoction (FZYGHX) reduces liver injury in carbon tetrachloride (CCl_4)-induced mice. A. Experimental design. B. Effects of FZYGHX on body weight. C. Liver index. D, E. Serum alanine aminotransferase (ALT) and aspartate aminotransferase (AST) levels. Data are presented as means \pm standard deviations (SD) (n=10). ***P<0.001 vs. control group; #P<0.05, ##P<0.01, ###P<0.001 vs. CCl_4 group.

disease databases were considered potential therapeutic targets. A compound-target (C-T) interaction network was constructed using Cytoscape 3.9.1. Gene Ontology (GO) and Kyoto Encyclopedia of Genes and Genomes (KEGG) pathway enrichment analyses were performed

Table 1. Analysis of the composition of the FZYGHX decoction

Latin name	Family	English name	Chinese name	Grams, g	Used part
Astragali Radix	Leguminosae	Milkvetch Root	Huangqi®	20	Roots
Atractylodis Macrocephalae Rhizoma	Asteraceae	Largehead Atractylodes Rhizome	Baizhu ²	15	Rhizome
Artemisiae Scopariae Herba	Asteraceae	Capillary Wormwood Herb	Yinchen [®]	10	Dry aboveground portion
Coicis Semen	Gramineae	Jobstears Seed	Yiyiren ⁴	12	Fruit seeds
Curcumae Rhizoma	Zingiberaceae	Acruginous Turmeric Rhizome	Ezhu [®]	10	Roots and rhizomes
Salviae Miltiorrhizae Radix Et Rh	Lamiaceae	Dan-Shen Root	Danshen [®]	15	Roots and rhizomes
Raphani Semen	Cruciferae	Radish Seed	Laifuzi [®]	10	Dry mature seeds
Ostreae Concha	Ostreidae	Common Oyster Shell	Muli [®]	15	Conch
Aurantii Fructus	Rutaceae	Immature Trifoliate-orange Fruit	Zhiqiao [®]	10	Dried young fruit
Glycyrrhiza uralensis Fisch	Legumes	Licorice	Gancao [®]	5	Dry roots and rhizomes

① Astragalis Radix: Derived from the dried roots of Astragalus membranaceus (Fisch.) Bge. var. mongholicus (Bge.) Hsiao or Astragalus membranaceus (Fisch.) Bge. ② Atractylodis Macrocephalae Rhizoma: Derived from the dried rhizomes of Atractylodes macrocephala Koidz. ③ Artemisiae Scopariae Herba: Derived from the dried aboveground parts of Artemisia scoparia Waldst. et Kit. or Artemisia capillaris Thunb. ④ Coicis Semen: Derived from the dried ripe seeds of Coix lacryma-jobi L. var. ma-yuen (Roman.) Stapf. ⑤ Curcumae Rhizoma: Derived from the dried rhizomes of Curcuma phaeocaulis Val., Curcuma kwangsiensis S. G. Lee et C. F. Liang, or Curcuma wenyujin Y. H. Chen et C. Ling. ⑥ Salviae Militorrhizae Radix Et Rhizoma: Derived from the dried roots and rhizomes of Salvia militorrhizae Bge. ⑦ Raphani Semen: Derived from the dried ripe seeds of Raphanus sativus L. ⑧ Ostreae Concha: Derived from the shells of Ostreae gigas Thunberg, Ostrea talienwhanensis Crosse, or Ostreae rivularis Gould. ⑨ Aurantii Fructus: Derived from the dried immature fruits of Citrus aurantium L. and its cultivars. ⑩ Glycyrrhizae uralensis: Derived from the dried roots and rhizomes of Glycyrrhizae uralensis: Fisch.

via the DAVID database. Enrichment results were visualized using OmicShare tools to predict biological functions and signaling pathways modulated by FZYGHX.

Immunofluorescence

Immunofluorescence (IF) staining was performed following standard protocols. Tissue sections were incubated overnight at 4°C with primary antibodies against claudin-1 (1:100, Proteintech, 28674-1-AP), occludin (1:100, Proteintech, 27260-1-AP), and ZO-1 (1:100, Proteintech, 21773-1-AP). Sections were then incubated with CoraLite594-conjugated secondary antibodies, and nuclei were counterstained with DAPI. Fluorescence images were captured using a DMi8 fluorescence microscope (Leica, Germany).

In vivo intestinal permeability assay

Intestinal barrier integrity was evaluated using the FITC-dextran permeability assay [8]. After a 12-hour fast, mice were gavaged with FITC-dextran (4 kDa, 600 mg/kg; Sigma, #FD4). Four hours post-gavage, blood was collected via tail vein under light-protected conditions and anticoagulated with heparin. Plasma was isolated via centrifugation (2,000×g, 10 min), and fluorescence intensity was measured at 490/520 nm. Concentrations were determined using plasma-based standard curves.

Western blot analysis

Hepatic protein expression was assessed via Western blotting. Equal amounts of protein (20) µg/lane) were separated on 10-15% SDS-PAGE gels and transferred to PVDF membranes (Solarbio, YA1701). Membranes were blocked with 5% nonfat milk in TBST for 2 h and incubated overnight at 4°C with the following primary antibodies: TLR4 (Bioss, BS-20594R), p-JNK (ZEN-BIOSCIENCE, 340810), JNK1/ 2/3 (ZEN-BIOSCIENCE, R24780), p-ERK1/2 (ZEN-BIOSCIENCE, R380698), ERK1/2 (ZEN-BIOSCIENCE, 343830), p-p38 (Proteintech, 28796-1-AP), p38 (Proteintech, 80821-2-RR), ΙκΒα (Proteintech, 80019-1-RR), p-p65 (Proteintech, 82335-1-RR), p65 (Proteintech, 80979-1-RR), and GAPDH (Servicebio, GB-15004). After washing, membranes were incubated with HRP-conjugated anti-rabbit IgG secondary antibodies (Servicebio, GB23303) and visualized using enhanced chemiluminescence (ECL) reagent. Bands were imaged using a GeneGnome5 system (UK) and quantified with ImageJ software, normalized to GAPDH.

Quantitative real-time PCR (qPCR)

Total RNA or DNA was extracted from liver tissues. For RNA samples, reverse transcription was performed to synthesize cDNA. Purified cDNA was used in qPCR reactions. Primers and fluorescent probes were designed to specifi-

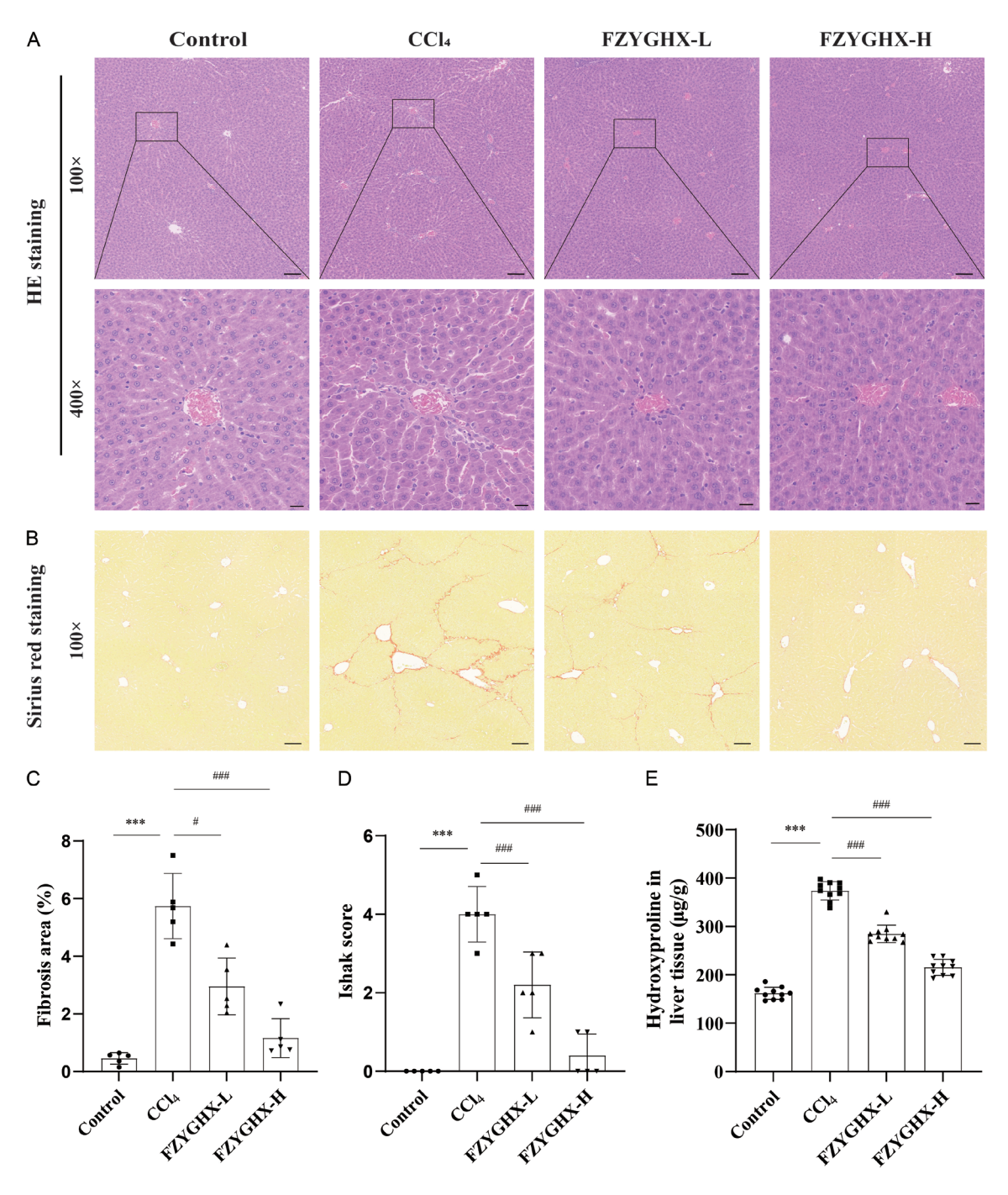


Figure 2. Fuzheng Yanggan Huaxian Decoction (FZYGHX) alleviates hepatic fibrosis in a carbon tetrachloride (CCl_4)-induced liver fibrosis mice. A. Representative liver histology by H&E staining in control, CCl_4 , FZYGHX-L, and FZYGHX-H groups (magnification: ×100, ×400). B. Sirius red staining showing collagen deposition (magnification: ×400). C. Semiquantification of Sirius red-stained areas using ImageJ (% of total area). D. Fibrosis score based on the Ishak system. E. Hydroxyproline (Hyp) content in liver tissues. Data are presented as means \pm SD (n=10). #P<0.05, ##P<0.01, ###P<0.001 vs. CCl_4 group.

cally target the genes of interest. Reaction mixtures included primers, probes, DNA template, polymerase, and buffer. Thermal cycling includ-

ed denaturation, annealing, extension, and fluorescence detection, as specified by the qPCR kit protocol.

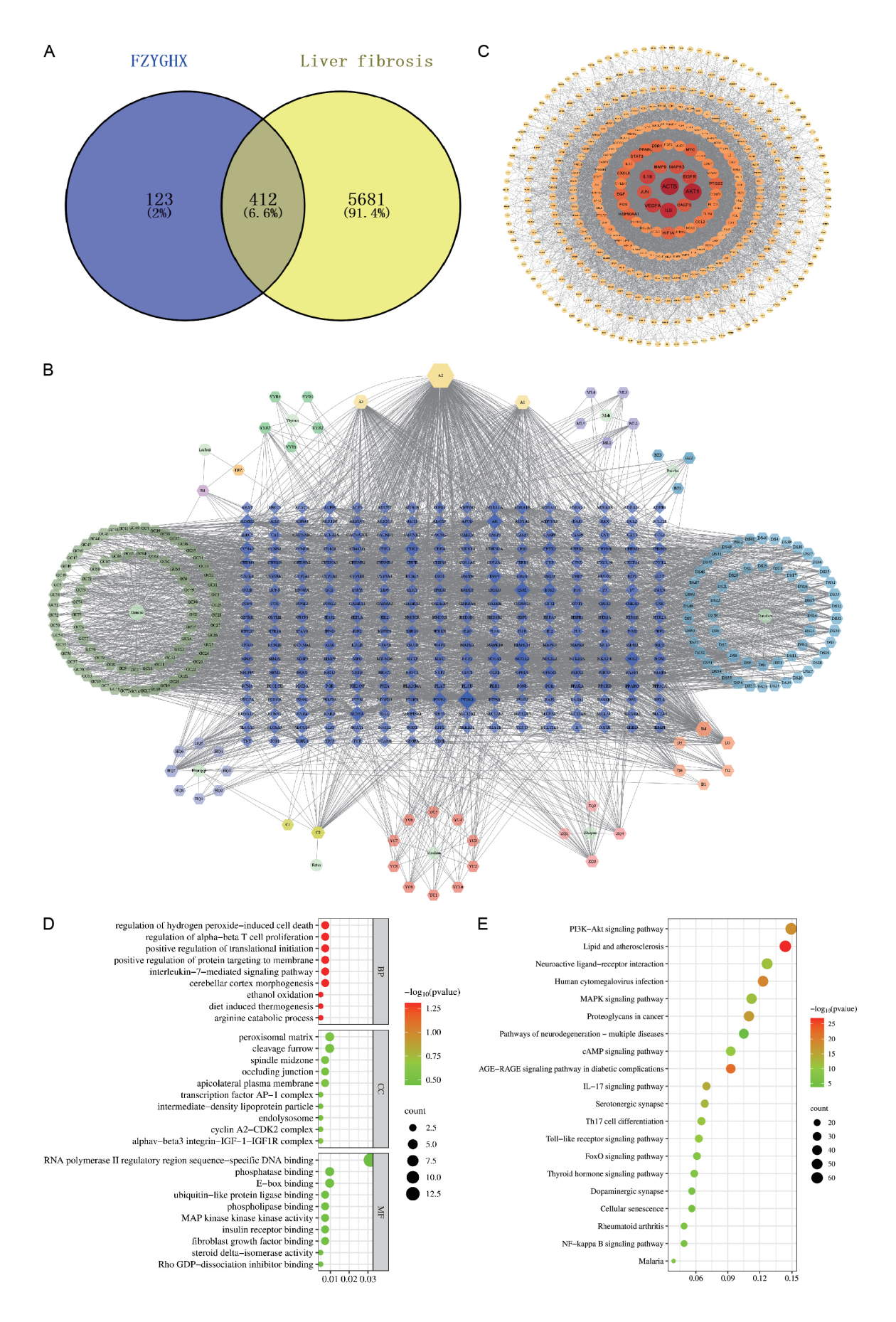


Figure 3. Network pharmacology analysis of the antifibrotic mechanism of Fuzheng Yanggan Huaxian Decoction (FZYGHX). A. Venn diagram showing 412 overlapping targets between FZYGHX and liver fibrosis. B. Herb-compound-target interaction network. Light green hexagons: herbs; orange circles: compounds; blue squares: target genes. C. Protein-protein interaction network of potential targets. D. Kyoto Encyclopedia of Genes and Genomes enrichment of key signaling pathways. E. Gene Ontology enrichment analysis. BP, biological process; CC, cellular component; MF, molecular function.

Statistical analysis

Data are presented as means ± standard deviation (SD). Normality and homogeneity of variance were assessed using the Shapiro-Wilk and Levene's tests, respectively. For comparisons among three or more groups, one-way ANOVA followed by Tukey's post hoc test was used. For two-group comparisons, Student's t-test was applied after verifying parametric assumptions. Multiple comparisons were adjusted using the Benjamini-Hochberg correction where appropriate. Statistical significance was set at P<0.05, with exact *p* values reported to two decimal places. Analyses were performed using SPSS 19.0 (IBM, USA).

Results

Effects of FZYGHX on CCI₄-induced hepatic injury

Following 8 weeks of intervention, CCl₄ administration significantly suppressed body weight gain compared to controls (**Figure 1B**) and was accompanied by reduced activity and appetite. FZYGHX treatment alleviated these clinical symptoms. Elevated hepatosomatic index and serum ALT/AST levels confirmed CCl₄-induced hepatotoxicity (**Figure 1C-E**). Notably, FZYGHX reversed these changes in a dose-dependent manner (P<0.01), indicating clear hepatoprotective effects.

FZYGHX attenuates CCI₄-induced liver fibrosis in vivo

Liver histopathology was assessed via H&E and Sirius red staining. The CCl₄ group showed disrupted hepatic architecture, fibroblast proliferation, inflammatory infiltration, periportal biliary hyperplasia, and cholestasis. FZYGHX treatment ameliorated these pathological features in a dose-dependent manner (**Figure 2A**). Sirius red staining revealed extensive collagen deposition and fibrotic septa formation in CCl₄-treated livers, which were markedly reduced by FZYGHX - especially in the

high-dose group, where hepatic structure approached that of controls (**Figure 2B-D**). Consistently, Hyp content was significantly decreased by FZYGHX (P<0.001; **Figure 2E**).

Identification of potential antifibrotic targets via network pharmacology

Network pharmacology analysis identified 412 overlapping antifibrotic targets among 535 differentially expressed genes (DEGs) associated with FZYGHX (Figure 3A). An herb-compound-target interaction network comprising 185 compounds was constructed (Figure 3B, 3C). GO and KEGG enrichment analyses revealed enrichment in MAPK, TLR, NF-kB, IL-17, Th17 cell differentiation, and PI3K-Akt pathways (Figure 3D, 3E). Based on their established roles in fibrogenesis, the MAPK/TLR/NF-kB pathways were prioritized for experimental validation.

FZYGHX suppresses inflammation in fibrotic livers

Immunofluorescence analysis of F4/80 (a Kupffer cell marker) showed marked upregulation in CCl_4 -treated mice, which was significantly reduced by FZYGHX, particularly at high doses (**Figure 4A**, **4B**). Hepatic pro-inflammatory cytokines IL-6 (**Figure 4C**) and TNF- α (**Figure 4D**) were elevated in the model group and reduced by 25-40% after FZYGHX treatment. In contrast, anti-inflammatory IL-10 levels (**Figure 4E**), which were suppressed by CCl_4 , were restored by FZYGHX. These results demonstrate that FZYGHX exerts potent anti-inflammatory effects during hepatic injury.

FZYGHX restores intestinal barrier integrity in CCI_a -induced liver fibrosis

Intestinal mucosal barrier function relies on TJ proteins such as ZO-1, claudin-1, and occludin. Immunofluorescence revealed substantial loss of these proteins in the colons of CCl₄-treated mice (**Figure 5A**), which was effectively reversed by FZYGHX in a dose-dependent

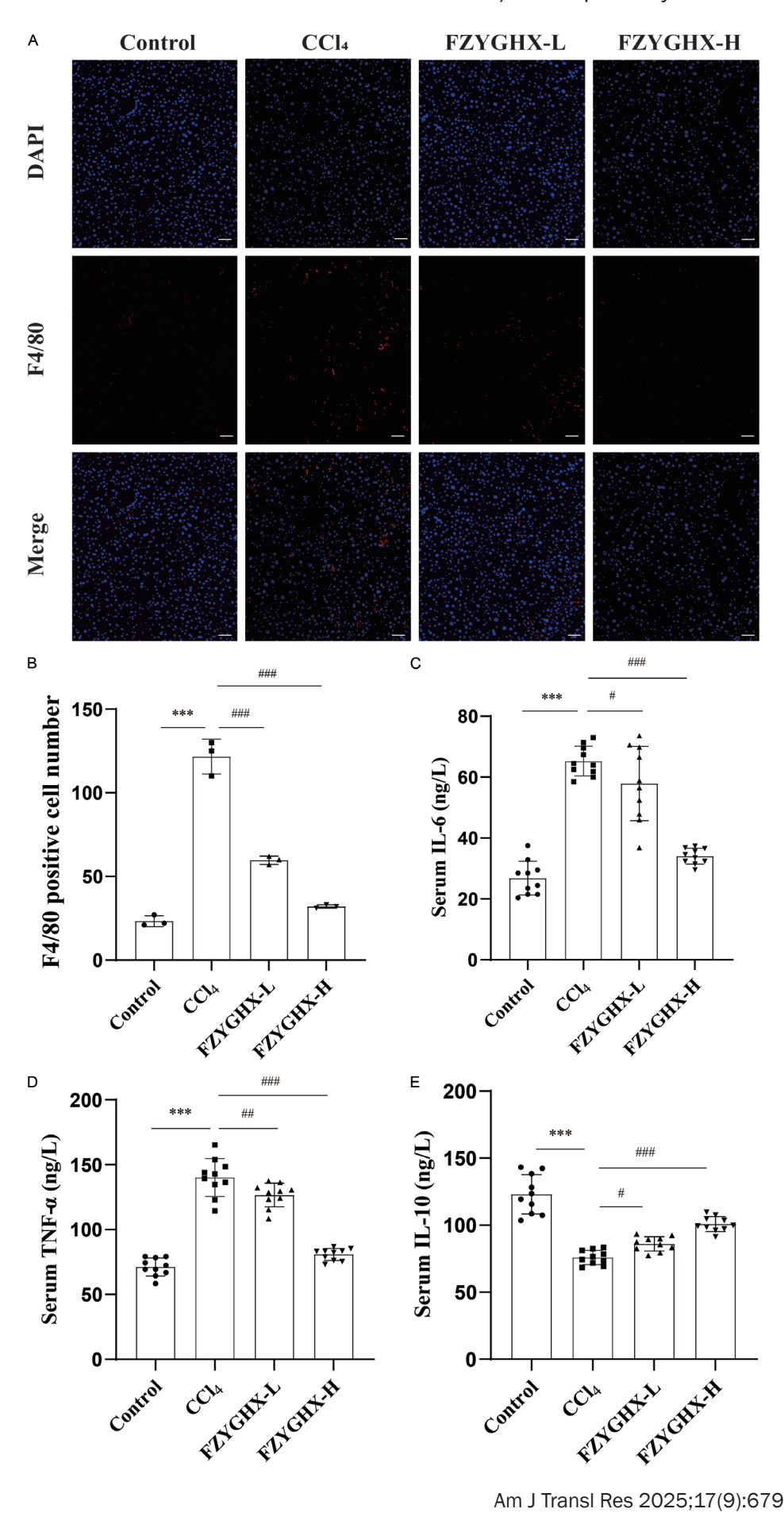


Figure 4. Fuzheng Yanggan Huaxian Decoction (FZYGHX) ameliorates inflammation in carbon tetrachloride (CCl₄)-induced liver fibrosis. A. Representative immunofluorescence staining of F4/80 $^{\circ}$ Kupffer cells (magnification: ×200). B. Quantification of F4/80 $^{\circ}$ cells (n=3). C-E. Serum levels of interleukin-6 (IL-6), interleukin-10 (IL-10), and tumor necrosis factor-alpha (TNF-α). Data are presented as means \pm SD. ***P<0.001 vs. control group; #P<0.05, ##P<0.01, ###P<0.001 vs. CCl₄ group.

manner. Barrier dysfunction led to elevated serum LPS levels (~70% increase in the model group). FZYGHX reduced serum LPS by 20-30% (**Figure 5B**) and normalized hepatic LPS-binding protein (LBP) levels, which were increased by 60% in fibrotic mice but decreased by 20-30% post-treatment (**Figure 5C**, **5D**). FITC-dextran permeability assays further confirmed these findings, showing a 70% increase in plasma FITC-dextran in CCl_4 -treated mice, which was attenuated by 20-35% following FZYGHX treatment (**Figure 5E**).

FZYGHX inhibits TLR4-MAPK/NF-κB signaling in hepatic fibrosis

Mechanistic studies showed that CCl_4 exposure activated TLR4 signaling and downstream effectors, as evidenced by increased phosphorylation of JNK, ERK, and p38 MAPKs, degradation of IκBα, and phosphorylation of the NF-κB subunit p65 (P<0.05, **Figure 6**). FZYGHX treatment significantly suppressed TLR4 expression and attenuated activation of the MAPK and NF-κB pathways (all P<0.05).

Discussion

Chronic liver diseases elicit sustained inflammatory responses that drive progressive fibrosis and ultimately lead to cirrhosis [9, 10]. Cirrhosis substantially increases the risk of severe complications, including liver failure, esophageal varices, hepatic encephalopathy, ascites, and HCC [11]. Despite growing efforts, early diagnosis and effective treatment of hepatic fibrosis remain global challenges [12]. Although recent research emphasizes noninvasive diagnostic strategies, the development of effective antifibrotic therapeutics is urgently needed. In line with the preventive principles of TCM, our findings demonstrate that FZYGHX attenuates hepatic fibrosis and delays its progression to cirrhosis and HCC (Figure 7).

Clinically, FZYGHX is known to resolve hepatic stagnation and improve blood circulation, with demonstrated efficacy in managing early-stage fibrosis and cirrhosis. Preclinical and clinical

evidence increasingly supports its hepatoprotective properties, particularly in reversing fibrosis, although the underlying mechanisms remain incompletely defined.

In this study, retro-orbital blood sampling enabled the quantification of liver enzymes (ALT/AST), while H&E and Sirius red staining were used for histopathological evaluation. FZYGHX treatment improved multiple fibrosis-associated parameters, including normalization of liver function markers, reduced hepatosomatic index, inhibition of collagen deposition, and attenuation of histological fibrosis severity.

Disruption of the intestinal mucosal barrier and subsequent microbial translocation are recognized contributors to hepatic fibrogenesis [13, 14]. Intestinal dysbiosis impairs epithelial barrier integrity, promoting the translocation of microbial products, which in turn exacerbate hepatic inflammation, injury, and fibrosis, ultimately progressing to cirrhosis [15, 16]. Fouts et al. [17] demonstrated significant intestinal dysbiosis and bacterial overgrowth during CCl₄-induced liver fibrosis, reinforcing the role of the gut-liver axis in disease pathogenesis.

The intestinal barrier comprises a monolayer of epithelial cells that regulates nutrient absorption while preventing luminal antigens, toxins, and pathogens from entering systemic circulation. This selective barrier operates via transcellular and paracellular routes, the latter of which is governed by apical junctional complexes, including TJs, adherens junctions, and desmosomes [15, 16]. TJs, in particular, regulate paracellular permeability through two distinct pathways: a "pore" pathway controlled by claudins and a "leak" pathway regulated by occludin [17].

In this study, immunofluorescence analysis revealed that FZYGHX significantly upregulated the expression of TJ proteins (ZO-1, claudin-1, and occludin) in CCl₄-treated mice, indicating restoration of intestinal barrier integrity. Impairment of this barrier typically leads to

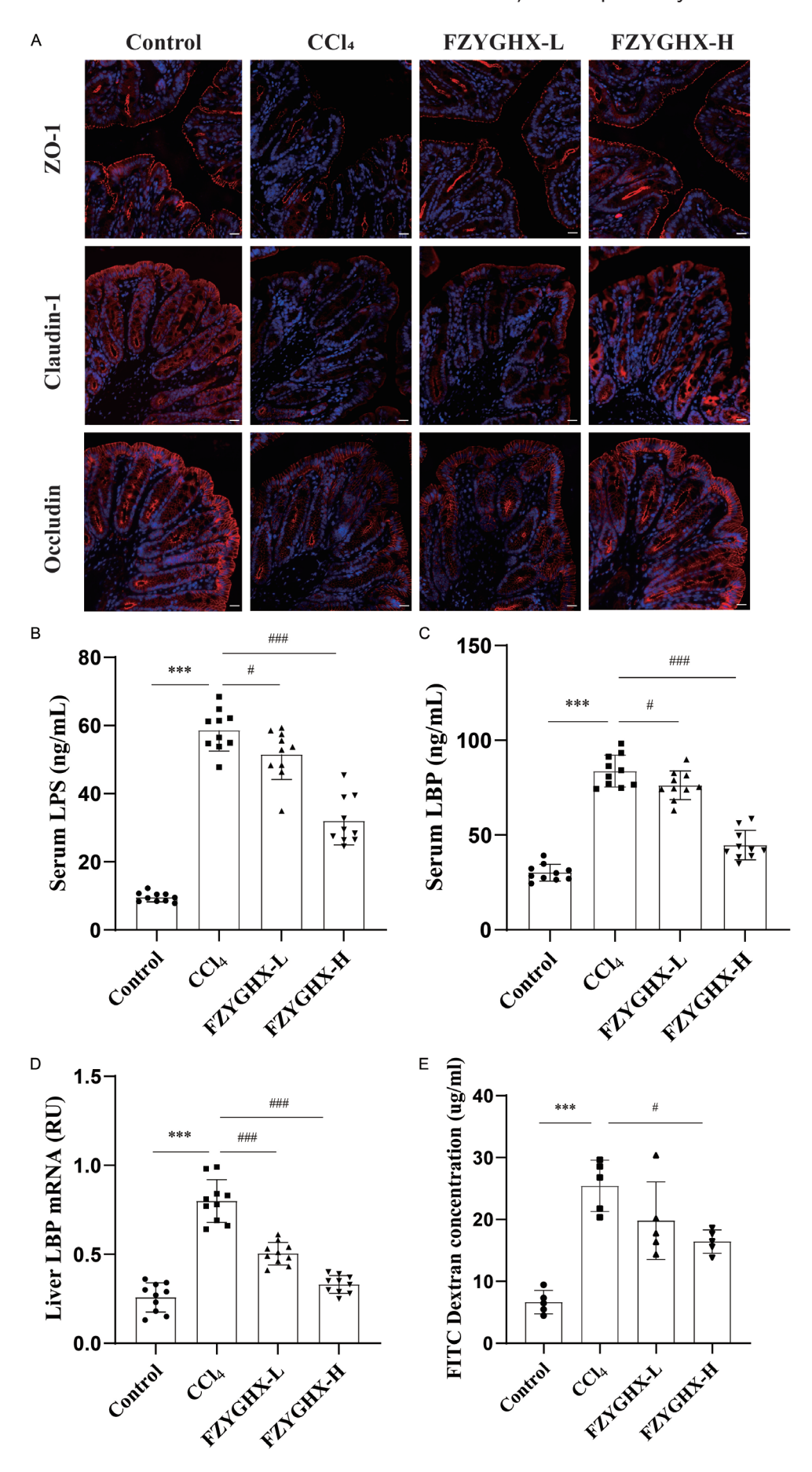


Figure 5. Fuzheng Yanggan Huaxian Decoction (FZYGHX) protects against carbon tetrachloride (CCl_4)-induced intestinal barrier dysfunction. A. Representative immunofluorescence images showing Claudin-1, Occludin, and ZO-1 expression in colonic tissues (magnification: ×400). B, C. Serum levels of lipopolysaccharide (LPS) and LPS-binding protein (LBP). D, E. FITC-dextran assay measuring intestinal permeability 4 hours after gavage with 4-kDa FITC-dextran (n=5). Data are presented as means \pm SD. ***P<0.001 vs. control group; #P<0.05, ###P<0.001 vs. CCl₄ group.

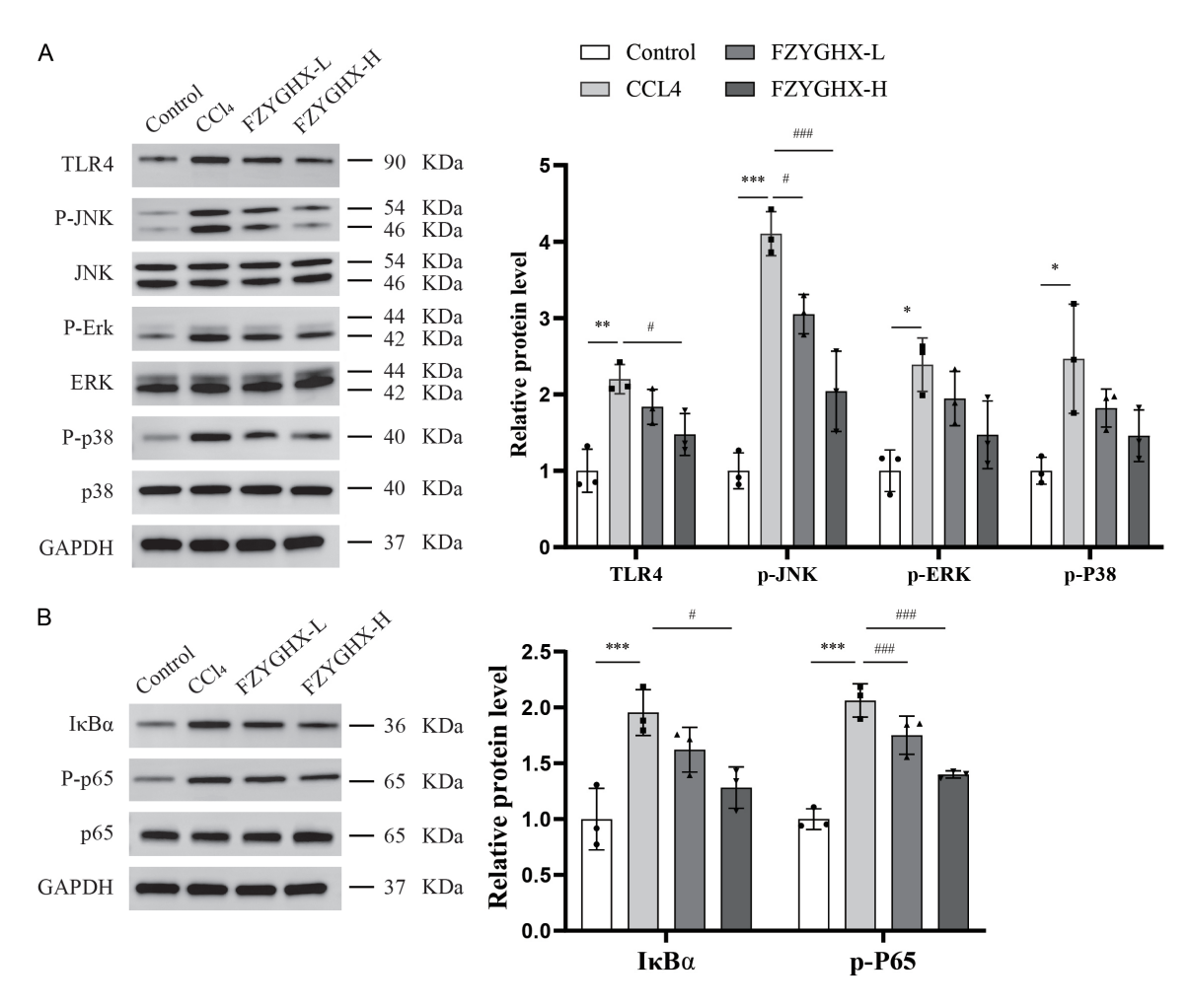


Figure 6. FZYGHX Fuzheng Yanggan Huaxian Decoction (FZYGHX) inhibits the TLR4-MAPK-NF- κ B signaling pathway in vivo. A. Western blot analysis of TLR4 and MAPK pathway-related proteins and their phosphorylated forms in liver tissue. B. Expression of I κ Bα and phosphorylated p65 in liver tissue. Data are presented as means \pm SD. *P<0.05, **P<0.01, ***P<0.001 vs. control group; #P<0.05, ##P<0.001 vs. CCl₄ group. JNK, c-Jun N-terminal kinase; P-JNK, Phosphorylated c-Jun N-terminal kinase; ERK, extracellular signal-regulated kinase; P-ERK, phosphorylated extracellular signal-regulated kinase; p38, p38 mitogen-activated protein kinase; P-p38, phosphorylated p38 mitogen-activated protein kinase; GAPDH, glyceraldehyde 3-phosphate dehydrogenase.

increased intestinal permeability and the translocation of bacterial components such as LPS and bacterial DNA [18, 19], resulting in endotoxemia and systemic inflammation. Our results showed elevated serum LPS and hepatic LBP levels in ${\rm CCl_4}$ -treated mice, both of which were dose-dependently normalized by FZYGHX. These effects were accompanied by reductions in F4/80 $^{+}$ Kupffer cells and serum

IL-6/TNF- α ratios, indicating mitigation of systemic inflammation and endotoxemia. Importantly, the concurrent upregulation of TJ proteins suggests that intestinal barrier repair plays a key role in the anti-inflammatory effects of FZYGHX.

CCl₄-induced gut barrier disruption and dysbiosis were further linked to elevated levels of pro-

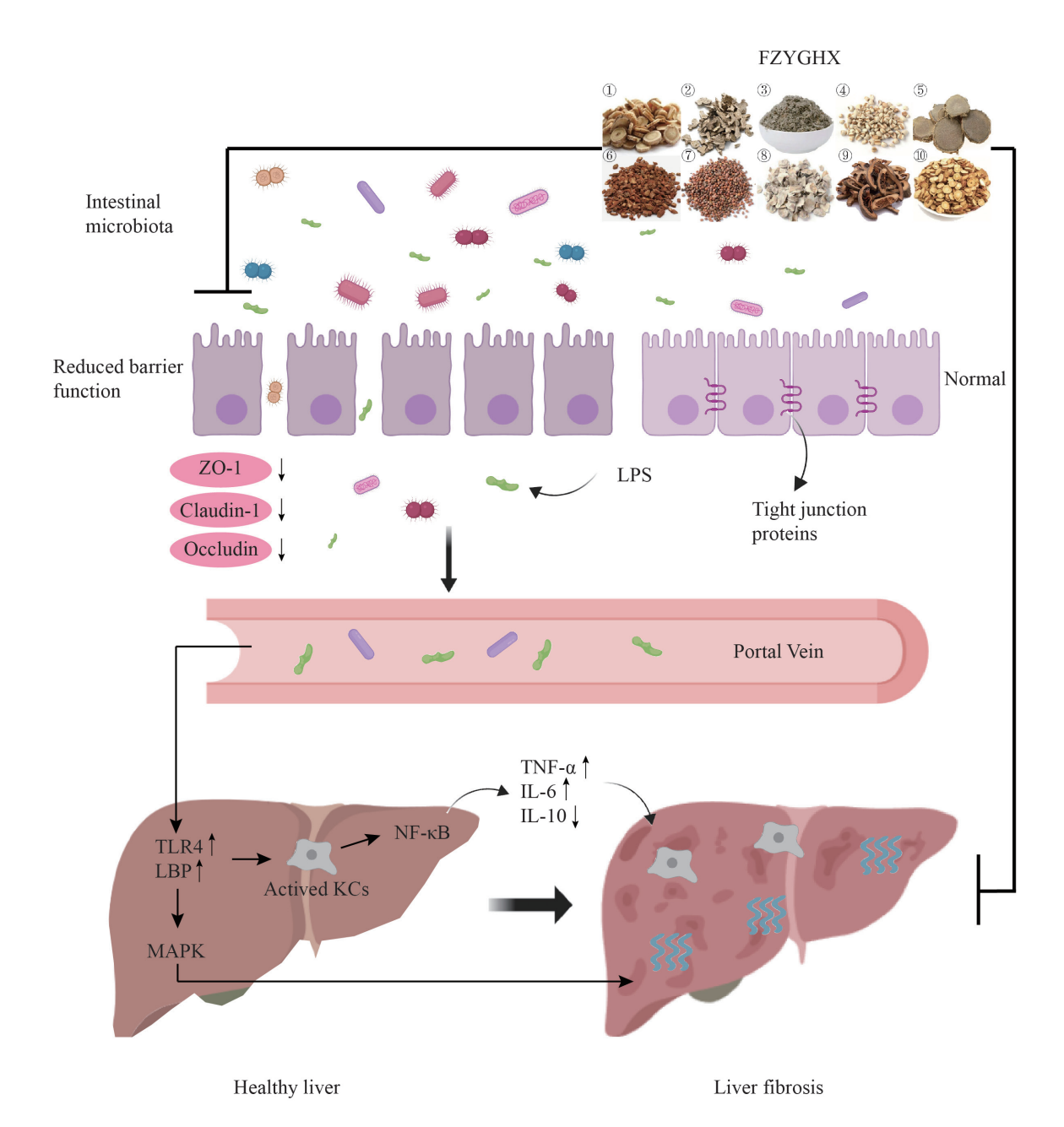


Figure 7. Schematic diagram of the proposed mechanisms by which Fuzheng Yanggan Huaxian Decoction (FZYGHX) inhibits carbon tetrachloride (CCl_4)-induced liver fibrosis. The hepatoprotective effect of FZYGHX may involve inhibition of the TLR4-MAPK-NF-κB signaling axis, restoration of intestinal barrier integrity, and suppression of systemic inflammation. ZO-1, zonula occludens-1; LPS, lipopolysaccharide; TNF-α, tumor necrosis factor alpha; IL-6, interleukin 6; IL-10, interleukin 10; LBP, LPS-binding protein; KCs, kupffer cells.

inflammatory cytokines, such as IL-6 and TNF- α , which promote liver injury and dysfunction [19-22]. NF- κ B is a central regulator of this inflammatory cascade, driving the nuclear translocation of p65 and the transcription of IL-1 β , IL-6, and TNF- α [23, 24]. FZYGHX treatment significantly suppressed serum cytokine elevations and inhibited NF- κ B activation.

Moreover, FZYGHX also blocked NF- κ B p65 nuclear translocation in CCL $_4$ -induced injury models, supporting its anti-inflammatory mechanism via NF- κ B inhibition.

TLR4 plays a pivotal role in initiating innate immune responses and activating the NF-κB pathway, ultimately promoting systemic inflam-

mation through the release of proinflammatory cytokines [25]. Mechanistically, FZYGHX down-regulated TLR4 expression and suppressed its downstream signaling cascades, including MAPK (p38, ERK, JNK) and NF-κB pathways. The CCl₄-induced phosphorylation of JNK and p38, which are known mediators of mitochondrial dysfunction and apoptosis [26], was also significantly attenuated by FZYGHX. These findings suggest that inhibition of the TLR4-MAPK-NF-κB axis is a core mechanism through which FZYGHX exerts hepatoprotective effects against fibrosis.

This study has several limitations. First, while the TLR4-MAPK/NF-kB axis was validated through in vivo experiments, the lack of cellspecific modulation, such as hepatocyte-specific TLR4 knockout, prevents establishing causal relationships. Second, the multi-component nature of FZYGHX decoction complicates attributing therapeutic effects to individual bioactive compounds, necessitating further compound isolation and synergy studies. Third, although intestinal barrier dysfunction was implicated, the spatial dynamics of gut-liver crosstalk and specific microbiota signatures remain uncharacterized. Finally, the CCI,-induced mouse model does not fully replicate human fibrotic progression heterogeneity, requiring validation in clinical cohorts with staged liver fibrosis.

Future research should focus on single-cell RNA sequencing of fibrotic liver tissues to better understand the roles of non-parenchymal cells in TLR4-MAPK-NF-kB signaling. Systems pharmacology approaches integrating ADMET screening and target fishing may identify the core active compounds in FZYGHX for optimization. Additionally, studying FZYGHX-modulated gut microbiota metabolites and their interactions with GPR41/TGR5 receptors could uncover barrier repair mechanisms. Finally, randomized controlled trials should evaluate FZYGHX's efficacy in NAFLD/HBV-related fibrosis subgroups with serum LPS/TLR4 biomarker monitoring.

In conclusion, this study demonstrates that FZYGHX alleviates CCl₄-induced liver fibrosis through anti-inflammatory activity and restoration of the intestinal mucosal barrier. The therapeutic effects are primarily mediated via inhibition of the TLR4-MAPK-NF-κB signaling pathway. These results provide compelling evi-

dence supporting the use of TCM-based strategies for the treatment of hepatic fibrosis and highlight FZYGHX as a promising therapeutic candidate for liver fibrosis management.

Acknowledgements

We are grateful to the Yunnan Research Center for Traditional Chinese Medicine and Preventive Medicine for providing laboratory space and experimental guidance. This work was supported by Yunnan Fundamental Research Projects (Grant Nos. 202301AZ07-0001-039 and 202301AT070251) and Science and technology projects of key industries in colleges and universities in Yunnan Province "projects with self-proposed topics" (Grant Nos. FWCY-ZNT2024017).

Disclosure of conflict of interest

None.

Abbreviations

ALT, Alanine aminotransferase; ANOVA, Analysis of variance; AST, Aspartate aminotransferase; ELISA, Enzyme-linked immunosorbent assay; FZYGHX, Fuzheng Yanggan Huaxian Decoction; H&E, Hematoxylin and eosin; Hyp, Hydroxyproline; IF, Immunofluorescence; IHC, Immunohistochemistry; IL-6, Interleukin-6; IL-10, Interleukin-10; LBP, LPS-binding protein; LPS, Lipopolysaccharide; MAPK, Mitogenactivated protein kinase; NF-κB, Nuclear factor kappa B; qPCR, Quantitative real-time polymerase chain reaction; SD, Standard deviation; TJs, Tight junctions; TLR4, Toll-like receptor 4; TNF-α, Tumor necrosis factor-alpha; WB, Western blot; ZO-1, Zonula occludens-1.

Address correspondence to: Xia Chen, The First Affiliated Hospital of Yunnan University of Chinese Medicine, Kunming 650021, Yunnan, China. E-mail: DcChenx@163.com; Yong Qiu, Yunnan University of Chinese Medicine, Kunming 650500, Yunnan, China. E-mail: yong_Q5015@163.com

References

- [1] Hammerich L and Tacke F. Hepatic inflammatory responses in liver fibrosis. Nat Rev Gastroenterol Hepatol 2023; 20: 633-646.
- [2] Kisseleva T and Brenner D. Molecular and cellular mechanisms of liver fibrosis and its regression. Nat Rev Gastroenterol Hepatol 2021; 18: 151-166.

- [3] Albillos A, de Gottardi A and Rescigno M. The gut-liver axis in liver disease: pathophysiological basis for therapy. J Hepatol 2020; 72: 558-577.
- [4] Wang Y and Liu Y. Gut-liver-axis: barrier function of liver sinusoidal endothelial cell. J Gastroenterol Hepatol 2021; 36: 2706-2714.
- [5] Althagafy HS, Ali FEM, Hassanein EHM, Mohammedsaleh ZM, Kotb El-Sayed MI, Atwa AM, Sayed AM and Soubh AA. Canagliflozin ameliorates ulcerative colitis via regulation of TLR4/ MAPK/NF-κB and Nrf2/PPAR-γ/SIRT1 signaling pathways. Eur J Pharmacol 2023; 960: 176166.
- [6] Reagan-Shaw S, Nihal M and Ahmad N. Dose translation from animal to human studies revisited. FASEB J 2008; 22: 659-661.
- [7] Pi A, Jiang K, Ding Q, Lai S, Yang W, Zhu J, Guo R, Fan Y, Chi L and Li S. Alcohol abstinence rescues hepatic steatosis and liver injury via improving metabolic reprogramming in chronic alcohol-fed mice. Front Pharmacol 2021; 12: 752148.
- [8] Fagan KJ, Pretorius CJ, Horsfall LU, Irvine KM, Wilgen U, Choi K, Fletcher LM, Tate J, Melino M, Nusrat S, Miller GC, Clouston AD, Ballard E, O'Rourke P, Lampe G, Ungerer JPJ and Powell EE. ELF score ≥9.8 indicates advanced hepatic fibrosis and is influenced by age, steatosis and histological activity. Liver Int 2015; 35: 1673-1681.
- [9] Volynets V, Reichold A, Bárdos G, Rings A, Bleich A and Bischoff SC. Assessment of the intestinal barrier with five different permeability tests in healthy C57BL/6J and BALB/cJ mice. Dig Dis Sci 2016; 61: 737-746.
- [10] Friedrich-Rust M, Poynard T and Castera L. Critical comparison of elastography methods to assess chronic liver disease. Nat Rev Gastroenterol Hepatol 2016; 13: 402-411.
- [11] Herrmann E, de Lédinghen V, Cassinotto C, Chu WC, Leung VY, Ferraioli G, Filice C, Castera L, Vilgrain V, Ronot M, Dumortier J, Guibal A, Pol S, Trebicka J, Jansen C, Strassburg C, Zheng R, Zheng J, Francque S, Vanwolleghem T, Vonghia L, Manesis EK, Zoumpoulis P, Sporea I, Thiele M, Krag A, Cohen-Bacrie C, Criton A, Gay J, Deffieux T and Friedrich-Rust M. Assessment of biopsy-proven liver fibrosis by two-dimensional shear wave elastography: an individual patient data-based meta-analysis. Hepatology 2018; 67: 260-272.
- [12] Alder JK, Chen JJ, Lancaster L, Danoff S, Su SC, Cogan JD, Vulto I, Xie M, Qi X, Tuder RM, Phillips JA 3rd, Lansdorp PM, Loyd JE and Armanios MY. Short telomeres are a risk factor for idiopathic pulmonary fibrosis. Proc Natl Acad Sci U S A 2008; 105: 13051-13056.

- [13] Nie YM, Zhou WQ, Niu T, Mao MF, Zhan YX, Li Y, Wang KP, Li MX and Ding K. Peptidoglycan isolated from the fruit of Lycium barbarum alleviates liver fibrosis in mice by regulating the TGF-β/Smad7 signaling and gut microbiota. Acta Pharmacol Sin 2025; 46: 1329-1344.
- [14] Schnabl B and Brenner DA. Interactions between the intestinal microbiome and liver diseases. Gastroenterology 2014; 146: 1513-1524.
- [15] Suzuki T. Regulation of intestinal epithelial permeability by tight junctions. Cell Mol Life Sci 2013; 70: 631-659.
- [16] Odenwald MA and Turner JR. The intestinal epithelial barrier: a therapeutic target? Nat Rev Gastroenterol Hepatol 2017; 14: 9-21.
- [17] Fouts DE, Torralba M, Nelson KE, Brenner DA and Schnabl B. Bacterial translocation and changes in the intestinal microbiome in mouse models of liver disease. J Hepatol 2012; 56: 1283-1292.
- [18] De Minicis S, Rychlicki C, Agostinelli L, Saccomanno S, Candelaresi C, Trozzi L, Mingarelli E, Facinelli B, Magi G, Palmieri C, Marzioni M, Benedetti A and Svegliati-Baroni G. Dysbiosis contributes to fibrogenesis in the course of chronic liver injury in mice. Hepatology 2014; 59: 1738-1749.
- [19] Chen W, Zai W, Fan J, Zhang X, Zeng X, Luan J, Wang Y, Shen Y, Wang Z, Dai S, Fang S, Zhao Z and Ju D. Interleukin-22 drives a metabolic adaptive reprogramming to maintain mitochondrial fitness and treat liver injury. Theranostics 2020; 10: 5879-5894.
- [20] Raevens S, Van Campenhout S, Debacker PJ, Lefere S, Verhelst X, Geerts A, Van Vlierberghe H, Colle I and Devisscher L. Combination of sivelestat and N-acetylcysteine alleviates the inflammatory response and exceeds standard treatment for acetaminophen-induced liver injury. J Leukoc Biol 2020; 107: 341-355.
- [21] Saad KM, Shaker ME, Shaaban AA, Abdelrahman RS and Said E. The c-Met inhibitor capmatinib alleviates acetaminophen-induced hepatotoxicity. Int Immunopharmacol 2020; 81: 106292.
- [22] Chen W, Shen Y, Fan J, Zeng X, Zhang X, Luan J, Wang Y, Zhang J, Fang S, Mei X, Zhao Z and Ju D. IL-22-mediated renal metabolic reprogramming via PFKFB3 to treat kidney injury. Clin Transl Med 2021; 11: e324.
- [23] Huang GJ, Deng JS, Huang SS, Lee CY, Hou WC, Wang SY, Sung PJ and Kuo YH. Hepatoprotective effects of eburicoic acid and dehydroe-buricoic acid from Antrodia camphorata in a mouse model of acute hepatic injury. Food Chem 2013; 141: 3020-3027.
- [24] Wang Z, Hao W, Hu J, Mi X, Han Y, Ren S, Jiang S, Wang Y, Li X and Li W. Maltol improves APAP-

- induced hepatotoxicity by inhibiting oxidative stress and inflammation response via NF-κB and PI3K/Akt signal pathways. Antioxidants (Basel) 2019; 8: 395.
- [25] Lawrence T. The nuclear factor NF-kappaB pathway in inflammation. Cold Spring Harb Perspect Biol 2009; 1: a001651.
- [26] Tashiro S, Tanaka M, Goya T, Aoyagi T, Kurokawa M, Imoto K, Kuwano A, Takahashi M, Suzuki H, Kohjima M, Kato M and Ogawa Y. Pirfenidone attenuates acetaminophen-induced liver injury by suppressing c-Jun N-terminal kinase phosphorylation. Toxicol Appl Pharmacol 2022; 434: 115817.